

## Working group report: Heavy-ion physics and quark-gluon plasma

*Coordinators:* MUNSHI G MUSTAFA<sup>1</sup> and SUDHIR RANIWALA<sup>2</sup>

*Contributors:* T Awes<sup>3</sup>, B Rai<sup>4</sup>, R S Bhalerao<sup>5</sup>, J G Contreras<sup>6</sup>, R V Gavai<sup>5</sup>, S K Ghosh<sup>7</sup>, P Jaikumar<sup>8</sup>, G C Mishra<sup>9</sup>, A P Mishra<sup>4</sup>, H Mishra<sup>10</sup>, B Mohanty<sup>11</sup>, J Nayak<sup>11</sup>, J-Y Ollitrault<sup>12</sup>, S C Phatak<sup>4</sup>, L Ramello<sup>13</sup>, R Ray<sup>1</sup>, P K Sahu<sup>4</sup>, A M Srivastava<sup>4</sup>, D K Srivastava<sup>11,14</sup> and V K Tiwari<sup>15</sup>

<sup>1</sup>Theory Group, Saha Institute of Nuclear Physics, 1/AF Bidhan Nagar, Kolkata 700 064, India

<sup>2</sup>University of Rajasthan, Jaipur 302 004, India

<sup>3</sup>Oak Ridge National Laboratory, High Energy Physics, Oak Ridge, Tennessee 37831-6372, USA

<sup>4</sup>Institute of Physics, Sachivalaya Marg, Bhubaneswar 700 005, India

<sup>5</sup>Tata Institute of Fundamental Research, Homi Bhabha Road, Mumbai 400 005, India

<sup>6</sup>Departamento de Fisica Aplicada, CINVESTAV, Mérida, Yucatán, México and PH Division, Centre for European Nuclear Research, Geneva, Switzerland

<sup>7</sup>Department of Physics, Bose Institute, 93/1, A.P.C. Road, Kolkata 700 009, India

<sup>8</sup>Physics Division, Argonne National Laboratory, Argonne, IL 60439-4843, USA

<sup>9</sup>Sikkim Manipal Institute of Technology, Majitar, Rango-737132, East Sikkim, Sikkim

<sup>10</sup>Theory Division, Physical Research Laboratory, Navrangpura, Ahmedabad 380 009, India

<sup>11</sup>Variable Energy Cyclotron Centre, 1/AF Bidhan Nagar, Kolkata 700 064, India

<sup>12</sup>Service de Physique Théorique, CEA/DSM/SPhT, Unité de Recherche associée au CNRS, F-91191 Gif-sur-Yvette Cedex, France

<sup>13</sup>Università del Piemonte Orientale, Alessandria and INFN-Torino, Italy

<sup>14</sup>Van de Graff Laboratory, Nuclear Physics Division, Bhabha Atomic Research Centre, Trombay, Mumbai 400 085, India

<sup>15</sup>Physics Department, Allahabad University, Allahabad 211 002, India

E-mail: munshigolam.mustafa@saha.ac.in, raniwala@uorehep.ac.in

**Abstract.** This is the report of Heavy Ion Physics and Quark-Gluon Plasma at WHEPP-09 which was part of Working Group-4. Discussion and work on some aspects of quark-gluon plasma believed to have created in heavy-ion collisions and in early Universe are reported.

**Keywords.** Quantum chromodynamics; quark-gluon plasma; lattice gauge theory; hydrodynamics; susceptibility; flow; AdS/CFT;  $J/\psi$ -suppression; screening; jet quenching; color superconductor.

**PACS Nos** 12.38.Aw; 12.38.Mh; 12.39.-x; 24.85.+p; 25.75.-q

## **0. Introduction**

Soon after the discovery of quantum chromodynamics (QCD), it was conjectured that at high temperature  $T$  the color charge is screened [1] and the corresponding phase of the matter was named quark-gluon plasma (QGP). It is a special kind of plasma in which the electric charges are replaced by the color charges of quarks and gluons, mediating the strong interaction among them. Such a state of matter is expected to exist at extreme temperatures, above 150 MeV, or densities, above about 10 times normal nuclear matter density. These conditions could have existed in the early Universe for the first few microseconds after the Big Bang or in the interior of neutron stars.

The aim of the ongoing relativistic heavy-ion collision experiments is to explore the possible QGP phase of QCD. The essential difference in heavy-ion collisions over the nucleon–nucleon collisions is the dominance of the partonic-level description for essentially all momentum scales and over nuclear size distances. In order to describe the produced system as a state of matter it is necessary to establish that these non-hadronic degrees of freedom form a statistical ensemble. Therefore, the concepts such as temperature, chemical potential and flow velocity should apply and the system can be explained by an experimentally determined equation of state. In addition, experiments should eventually be able to determine the physical characteristics of the phase transition, viz., the critical temperature, the order of the phase transition, and the speed of sound along with the nature of underlying quasi-particles. To date such a description is provided by the lattice QCD (LQCD) calculations. Ultimately, one would expect to validate this by characterizing the QGP in terms of its experimentally observed properties. The commissioning of Relativistic Heavy Ion Collider (RHIC) at BNL and various experiments performed therein have ushered in a new era. These experiments have acquired data on Au+Au collisions at various energies, an essential  $p+p$  baseline data set, and a critical  $d+Au$  comparison. The analyses of these various systems have yielded a rich abundance of results.

There were non-overlapping talks and overlapping talks during WHEPP. The non-overlapping talks on this subject were focussed on the recent developments in LQCD, present status of experimental observations and the corresponding theoretical efforts, and certain aspects of future experiments, in understanding the properties of QGP produced in heavy-ion collisions. Details are reported in these proceedings.

1. Status of lattice QCD: Rajiv V Gavai
2. Results from STAR experiment at RHIC: Bedanga Mohanty
3. PHENIX overviews – Status of QGP: Terry Awes
4. Jets in ALICE: J Guillermo Contreras
5. Theoretical status of QGP: Jean-Y Ollitrault
6. High energy photons from relativistic heavy ion collider: Dinesh K Srivastava
7. On the structure and appearance of quarks stars: Prashanth Jaikumar

Recent numerical LQCD calculations have given us wealth of information on various thermodynamic properties at finite temperature and chemical potential. It has

now been established that there is only a cross-over [2] of normal hadronic matter to a state of deconfined quarks and gluons at temperature  $T_C \sim 200$  MeV. Moreover, the equation of state [2], various susceptibilities [3,4] and transport coefficients [5] have been obtained. It is also found that charmonium states remain bound at least up to  $T \sim 2T_C$  [6] and the behavior of temporal correlators in pseudoscalar and vector channels deviates significantly from the free behavior at  $T \sim 3T_C$  [7]. These analyses suggested that pseudoscalars and vectors resonances may exist above  $T_C$ .

Robust results from Au+Au at the BNL RHIC experiments have shown collective effects known as radial [8] and elliptic [9,10] flows, and a suppression of high- $p_T$  hadron spectra [10,11], which could possibly indicate the quenching of light quark and gluon jets [12]. The hydrodynamical description of the observed collective flow indicates that the matter produced at RHIC behaves like a near-perfect fluid [13]. On the other hand, the amount of jet quenching might depend on the state of matter of the fireball, i.e., QGP or a hot hadron gas. There are extensive theoretical efforts in understanding the effect of the medium on jet quenching [14–18] using collisional as well as radiative energy loss since the high energy partons traveling through a medium will lose energy owing to the interactions in the medium. The measurement in RHIC [19] indicates excess direct photons over the next-to-leading order pQCD processes in RHIC and extensive theoretical efforts were made to understand these excess photons [20]. In astrophysical part the focus was to study and understand the *structure* of standard model at low energy and the *evolution* of the early Universe.

The working group activity was structured around review talks followed by discussions. The emphasis in this working group (IV) was to establish connection between the subject matter of the review talks in plenary sessions and some informal talks during discussion sessions, which led to the identification of relevant physics problems along with efforts to work them out. This working group IV was particularly interested in the following topics and relevant problems: (1) Charmonium suppression, (2) jet quenching and jet identification, (3) hydrodynamic description of elliptic flow, (4) susceptibilities and speed of sound in QGP, (5) possibility of bound states in QGP, (6)  $\phi$ -production at RHIC, (7) AdS/CFT – QCD/QGP and (8) neutrino emission from crystalline color superconducting quark matter.

In the next few sections we will briefly report the discussion held on these topics, and also the progress made on the relevant physics problems undertaken by the working group members.

## 1. Charmonium suppression

*L Ramello*

The latest results from CERN SPS fixed target experiments NA50 and NA60 about heavy quarkonia (mostly charmonium) production in  $p$ -nucleus collisions at 400 and 450 GeV and in In–In, Pb–Pb collisions at 158 GeV/nucleon are presented. For a historical overview of charmonium studies at SPS, see [21].

Experiments NA50 and NA60 share the same muon spectrometer which allows to trigger on dimuons emitted from charmonium and bottomonium decays, as well from the Drell–Yan process and open charm associated production. NA50 has three independent centrality detectors: an electromagnetic calorimeter, a multiplicity

detector and a zero-degree calorimeter (ZDC). NA60 retains the ZDC for centrality measurement and has a vertex magnet and a silicon pixel vertex spectrometer which allows matching between the muon tracks in the muon spectrometer and in the vertex spectrometer.

The recent NA50  $p$ - $A$  results at 450 and 400 GeV [22] allow (together with NA38 and NA3 data at 200 GeV) to determine the  $J/\psi$  nuclear absorption only from proton-induced reactions, without reference to S-U results. A value of  $\sigma_{\text{absorption}}(J/\psi) = 4.18 \pm 0.35$  mb is obtained. This in turn allows to calculate the expected  $J/\psi$  yield in Pb-Pb collisions at 158 GeV/nucleon and in S-U collisions at 200 GeV/nucleon. The centrality dependence in Pb-Pb is calculated with a Glauber model using the variable  $L$  (average path in nuclear matter) as a common parameter in  $p$ - $A$ , S-U, In-In and Pb-Pb collisions.

The NA50 ( $J/\psi$ /Drell-Yan) and ( $\psi'$ /Drell-Yan) cross-section ratios as a function of centrality are obtained from Pb-Pb data samples collected at 158 GeV per nucleon in the 1998 run and, under improved experimental conditions, in 2000 [23].

The  $J/\psi$  expected production extrapolated from  $p$ - $A$  data is then compared to the NA50 results in Pb-Pb collisions, as well as to the NA38 results for S-U reactions. A departure from normal nuclear absorption is observed for mid-central Pb-Pb collisions, with the suppression increasing with centrality. The three centrality variables give a consistent picture. On the other hand, peripheral Pb-Pb data and all S-U data are compatible with normal nuclear absorption. The  $\psi'$  has a significant absorption in  $p$ - $A$  collision, which is further increased by about a factor 3 both in S-U and Pb-Pb collisions. The  $J/\psi$  suppression has been studied as a function of  $p_T$ : the anomalous suppression is concentrated at low  $p_T$ . For  $p_T > 3.5$  GeV/c, the central-to-peripheral ratio  $R_{CP}$  becomes almost independent of the centrality range. The average square  $p_T$  (or equivalently the effective temperature) of the  $J/\psi$  first increases with centrality and then saturates in central Pb-Pb collisions.

The NA60 experiment has studied the centrality dependence of the  $J/\psi$  production in another system, namely In-In, at 158 GeV per nucleon [24]. The  $J/\psi$ /Drell-Yan ratio in In-In in three centrality bins compares well with NA50 Pb-Pb results, in the sense that anomalous suppression is seen also in In-In in the limited range of  $L$  accessible to this analysis. NA60 has presented more detailed (still preliminary) results by directly comparing the measured  $J/\psi$  sample with a theoretical distribution expected in the case of pure nuclear absorption. The onset of anomalous suppression in In-In is clearly seen in the range  $80 < N_{\text{part}} < 110$  ( $N_{\text{part}}$  being the number of participating nucleons), with saturation for larger values of  $N_{\text{part}}$ , up to about 200. Comparing the NA60 direct  $J/\psi$  analysis with NA38/NA50 results, it is evident that the three data sets do not overlap when plotted against  $L$ , while a rather good overlap is seen when they are plotted against  $N_{\text{part}}$ , as seen in figure 1.

The SPS data presented above and the PHENIX results [25] obtained with Au+Au and Cu+Cu collisions at RHIC (c.m. energy of 200 GeV/nucleon) have been compared with a few models [26-29], which attempt to describe data under different assumptions. Models have in general been tuned on  $p$ - $A$ , S-U and Pb-Pb SPS data and give predictions for In-In data and for RHIC Au-Au (Cu-Cu) data.

Model [26], based on  $\chi_C$  suppression in a percolation scenario, predicts an onset of the suppression at SPS in Pb-Pb collisions at  $N_{\text{part}} \sim 125$ , which agrees with

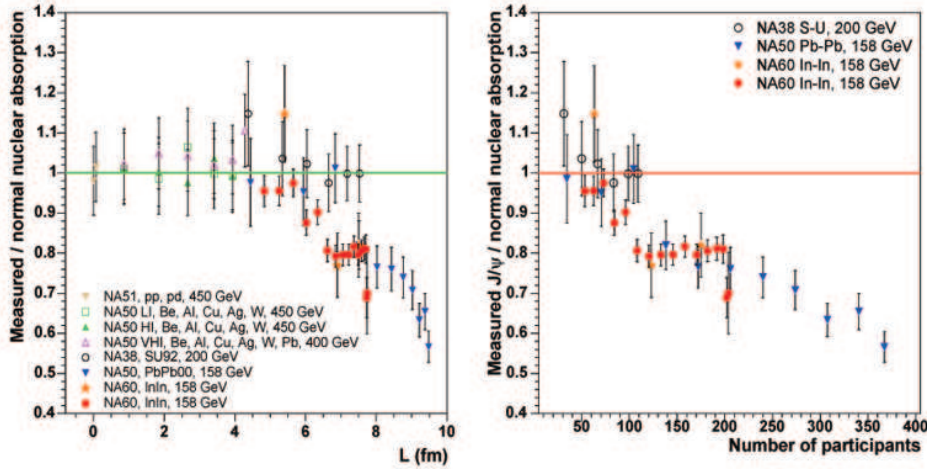


**Figure 1.** The S-U, In-In and Pb-Pb data points do not overlap in  $L$ , as seen in the left panel. The  $J/\psi$  suppression patterns for different interacting systems are in fair agreement with  $N_{\text{part}}$ .

NA50 data, and an onset in In-In collisions at  $N_{\text{part}} \sim 140$ , which disagrees with NA60 data (the onset in data is at  $N_{\text{part}} \sim 90$ ).

Model [27] contemplates charmonium suppression and regeneration in both QGP and hadron gas phases. At SPS only a small amount of regeneration is needed, and both NA50 and NA60 data are well described, except for In-In data at  $N_{\text{part}} > 160$  which are underpredicted. At RHIC 200 GeV c.m. energy in Au-Au collision, a substantial amount of regeneration is needed to describe data.

Model [28] includes nuclear absorption ( $\sigma_{\text{abs}} = 4.5$  mb) and comover absorption ( $\sigma_{\text{co}} = 0.65$  mb). SPS data for Pb-Pb collisions are well described, while those for In-In collision are slightly underpredicted: the ratio measured/expected (expected from normal nuclear absorption) for semi-central and central collisions is 0.80 in data without any centrality dependence, while it is 0.70 and decreasing with centrality in the model. The  $R_{AA}$  ratio at RHIC for Au-Au and Cu-Cu collisions at  $N_{\text{part}} \sim 300$  is largely underpredicted (0.10 vs. 0.35).

Model [29] has in fact two scenarios: the QGP scenario underpredicts the Au-Au PHENIX data, while the statistical coalescence model (valid for  $N_{\text{part}} > 100$ ) predicts a flat behavior vs.  $N_{\text{part}}$  and roughly agrees with PHENIX  $dN(J/\psi)/dy$ .

## 2. Jets

### 2.1 Jets in ALICE

*J G Contreras*

Jets, at the parton level, are cascades of quarks and gluons produced by a fast moving parton in a process called fragmentation. In the ALICE experiment, the fast partons are created as a product of hard scattering, where the incoming partons are provided by the collision of two extremely relativistic protons or nuclei. At the

detector level, jets are the highly collimated bundle of particles produced by the hadronization process of the partonic jet.

The fragmentation properties of a parton jet are influenced by its interaction with the medium, where the parton loses its energy in the QGP. This phenomenon is called jet quenching and it has been advocated to be an ideal probe of the QGP state created by the collision of two heavy ions at asymptotic energies [12]. Partonic jets from hard scattering are created before the QGP in the collision of two heavy ions. Hard scatterings and the evolution of fragmentation in vacuum can be quite reliably computed within pQCD. Any changes in the fragmentation process in the presence of QGP can be determined, in principle, from the measurement of jet quenching. There are some caveats in this approach. The experiments measure jets after hadronization, the effect of which cannot be calculated *a priori*, inhibiting a unique determination of the effect of QGP on the partons. However, there are models which assume (with certain confidence) that the influence of hadronization is small in certain regions of phase space. Also, lacking detailed understanding of the QGP state, the understanding of the interaction of a parton jet with a QGP is still in an evolutionary phase.

There have been attempts to understand the effect of the medium on the jet quenching due to the radiative energy loss [14–17], and recently also due to the collisional energy loss [18]. Furthermore, only the first approximation to radiative energy loss has been used, but a lot of theoretical work is under progress in this area. Notwithstanding these limitations, observation of jet quenching in RHIC data [11] has been used to ‘announce’ the creation of a QGP.

The experiments at RHIC have shown that there is jet quenching and that it is definitely a final state effect. It must be mentioned here that there is an inherent bias in leading particle analysis, which can be best eliminated by studying the complete jets. Further, it is desirable to study the QCD evolution of jet quenching. This can be best done by studying evolution of jet quenching with the hardness of the scale by comparing jet shapes in a wide kinematic domain. These steps lead to the ALICE experiment at the large hadron collider at CERN; to new problems, and also to new opportunities.

The physics reach of studying jets in the ALICE experiment has been reported in [30] and a brief overview is discussed here.

It is expected that under nominal conditions of LHC running, several tens of jets with energies below 15 GeV will be produced in each Pb–Pb event within the acceptance of ALICE. It is also expected that there will be jet(s) of 250 GeV for one month of data taking. The large charge particle multiplicity envisaged in the heavy-ion collision, in contrast to *pp* collision, will lead to several hundreds of GeV of energy deposition in one unit in the azimuth-rapidity space. The fluctuations in the average energy in a given cone are of the order of several tens of GeV and form a formidable background to observe jets.

The strategy planned for the ALICE experiment is to use smaller cones, and to search for the jets using particles whose energy lies above a given threshold and to iteratively subtract the background using a modified jet cone algorithm [31]. It has been shown that above 50–60 GeV of energy, jets and their spectra can be reliably reconstructed using this modified jet algorithm on the charged particles produced in the interaction and measured by the TPC.

Jet quenching affects certain properties of the jet-like amount of radiation outside a given cone, jet heating and the fragmentation function [15]. The various variables have relative merit, e.g. one variable (jet heating) does not evolve with the hardness of the interaction and cannot be used to test the QCD evolution of jet quenching, while remaining a good test of jet quenching at all hardness scales. In contrast, fragmentation function of jets offers a window to study the evolution of jet quenching with the hardness of the interaction.

In summary, jet shapes are ideal testbeds to study jet quenching phenomena. To use them it is mandatory to measure very low-energy particles and to understand with great precision the contribution from the underlying event and its fluctuation. ALICE fulfills all the requirements to perform these demanding measurements and extract from them the properties of jet quenching and thus increase our understanding of the QGP.

## *2.2 Flow coefficients and jet characteristics in heavy-ion collisions: New methods of jet identification*

*S C Phatak*

Identification of jets in heavy-ion collisions is an important and challenging problem because modification of jet properties is expected to give information on possible formation of quark-gluon plasma during the collision process [14–18]. Jet quenching has already been observed [11], although the observation is somewhat indirect. In particular, these studies are basically the correlation studies between the energetic hadrons which are expected to be the hadrons produced in a jet. Detecting and identifying jets in heavy-ion collisions is an essential prerequisite to study jet quenching.

A new method for jet identification has been developed [32]. The method is based on the fact that the flow or Fourier coefficients for events containing jets have typical structure enabling identification of jet events and determining its opening angle and the number of particles. The even coefficients in back-to-back jets are observed to be larger.

The flow coefficients are Fourier coefficients of the azimuthal distribution of particles produced in heavy-ion collisions and are given by

$$v_{m,p_T}^2 = \int d\phi_1 d\phi_2 dp_{T1} dp_{T2} p_{T1} p_{T2} P(\phi_1) P(\phi_2) \cos m(\phi_1 - \phi_2). \quad (1)$$

Given the experimental distribution of particles, the flow coefficients are given by  $v_{m,p_T}^2 = \frac{1}{N^2} \sum_{i,j} p_{T,i} p_{T,j} \cos(\phi_i - \phi_j)$  where  $N$  is the number of particles in the event and  $p_{T,i}$  is the transverse momentum of  $i$ th particle. For uniformly distributed particles, all flow coefficients (except for  $m = 0$ ) vanish whereas for  $\delta$ -function distribution all coefficients are unity. Thus, for an event with a jet having a number of particles in a small azimuthal angle and the rest of the particles uniformly distributed,  $v_m$ s are expected to be abnormally large. This can be used to identify a jet and to determine the jet properties. We have shown that [33], if an event has jet particles distributed in a narrow cone of azimuthal angle, we have

$v_{m,p_T}^2 = \frac{N_j \langle p_T \rangle^2}{N^2} [1 - m^2 \sigma^2 + \mathcal{O}(m^4)]$  where  $\sigma$  is the variance of the  $\phi$ -distribution and  $\langle p_T \rangle$  is the average transverse momentum carried by a hadron in the jet. Thus  $N_j \langle p_T \rangle$  is the transverse momentum of the jet.

These expressions clearly suggest a method of obtaining jet properties from the flow coefficient. A linear fit to  $v_{m,p_T}^2$ , plotted as a function of  $m^2$  would yield the number of jet particles and jet  $p_T$  from the intercept on  $y$ -axis and  $\sigma$  from the slope.

Let us now consider the case of two back-to-back jets in a background of uniformly distributed particles. This case is of interest because we expect that a hard parton scattering would produce such jets having equal and opposite jet momenta. We expect that quenching of one of the jets would broaden one of the jets and/or produce more jet particles. Thus, the characteristics of the two back-to-back jets would be different. Further, in an extreme situation, the fast moving parton of one of the jets may be completely absorbed in the medium leading to removal of one of the jets. Assuming that the jet particles are distributed uniformly in the jet cone of the respective jets, we get

$$v_{m,p_T}^2 = \frac{1}{N^2} \left[ \langle p_{T,1} \rangle j_0 \left( \frac{m \Delta \phi_{j1}}{2} \right) + (-1)^m \langle p_{T,2} \rangle j_0 \left( \frac{m \Delta \phi_{j2}}{2} \right) \right]^2. \quad (2)$$

Here  $N_{ji}$  are the jet particles in the  $i$ th jet,  $\Delta \phi_i$  are the corresponding opening angles and  $\langle p_{T,i} \rangle$  the average transverse momenta of the respective jet particles. The presence of  $(-1)^m$  factor in the second term above implies odd-even staggering in  $v_m^2$ s. In particular, odd coefficients vanish for identical jets. This property would be useful in estimating the possible quenching of one of the jets. The method also works when transverse momentum is not measured and only the azimuthal angle of the particles is known.

The method was tested using simulations. Jet particles were simulated by adding certain number of particles distributed uniformly in a jet cone of  $\Delta \phi$  and having exponentially decreasing  $p_T$  distribution and added to HIJING events [34] adapted for LHC energies. Different values of the number of jet particles and jet opening angles were used for analysis. In the absence of any jet particles, the method yields  $v_{m,p_T}^2$  values smaller than  $0.05 \text{ GeV}^2$ . In case of the data with jet only, the method outlined above is able to extract correctly the number of jet particles, jet transverse momentum and jet opening angle.

### 3. Dissipative relativistic hydrodynamics

*R S Bhalerao*

Certain global features of the RHIC data on ultrarelativistic heavy-ion collisions have been successfully explained in the framework of the boost-invariant ideal hydrodynamics: The main characteristics of the observed elliptic flow ( $v_2$ ) are reasonably well described by ideal fluid dynamics, while requiring unreasonably large cross-sections in transport models. The ability of the former to reproduce both the elliptic flow and single-particle spectra for measured hadrons with  $p_T \leq 2 \text{ GeV}/c$  near midrapidity in minimum-bias collisions is considered as a significant finding

at RHIC. The dependence of the flow pattern on hadron masses further supports the hydrodynamical picture.

However, the short time-scale for equilibration is difficult to account for microscopically [35]. (It has been argued recently that plasma instabilities may provide a mechanism for fast thermalization.) Moreover, several features of the data clearly signal the breakdown of the ideal hydrodynamical description [36]: Hydrodynamic models seem to work for minimum-bias data but not for centrality-selected pion and antiproton data. Indeed, the pion data presented in figure 36 of [37] show that the measured  $v_2$  in central collisions overshoots the value obtained by a hydrodynamical computation,  $v_2(\text{data}) > v_2(\text{hydro})$ , contrary to the expectation that the  $v_2$  measurements saturate the hydrodynamical limit. See also figure 6 of [37] where the agreement between  $v_2(\text{data})$  and  $v_2(\text{hydro})$  is far from satisfactory. This indicates incomplete equilibration and/or importance of dissipative effects.

Hydrodynamic calculations have shown that  $v_2$  is independent of the system size for a given shape of the collision zone. This is a consequence of scale invariance of ideal hydrodynamics. However, incomplete equilibration breaks this scale invariance making  $v_2$  depend upon the system size. Certain dimensionless numbers like Mach number, Knudsen number and Reynolds number can be used to characterize the motion of the fluid, in particular its compressibility, degree of thermalization and importance of viscous effects. Estimating these numbers for Au–Au collisions at RHIC calls in question the assumption of local equilibrium and applicability of ideal hydrodynamics, and at the same time points to the need for dissipative relativistic hydrodynamic description of nucleus–nucleus collisions at RHIC.

#### **4. Susceptibilities and speed of sound in QGP in PNJL model**

*Sanjay K Ghosh, Tamal K Mukherjee, Munshi G Mustafa and Rajarshi Ray*

Susceptibility is the response of the system to an externally applied force. Quark number susceptibilities are the response of the quark number density to the variation of chemical potential. Lattice data on QCD thermodynamics, particularly recent study of higher-order susceptibilities [3,4] have provided valuable information and new insight about the properties of matter produced around and above the critical temperature,  $T_C$ . Perturbative QCD calculations fail to describe the details of these results. There are some model calculations to understand the physical picture of the structures in higher-order susceptibilities produced by those LQCD data. The hadron gas resonance model [38] describes the data well below  $T_C$  but fails for  $T > T_C$ . The recently proposed [39] scenario of colored bound states also compares the data. However, their comparison is still not completely satisfactory. In this work [39a] we try to understand the features and structures of the susceptibilities produced by LQCD within the model described below.

The thermal average of the Polyakov-loop can be considered to be the order parameter for deconfinement transition [40]. Hence a judicious use of the Polyakov-loop in effective models may prove to be of great advantage. On the other hand, the QCD inspired models, predominantly, the NJL model, has given rise to an interesting phase diagram in temperature and chemical potentials.

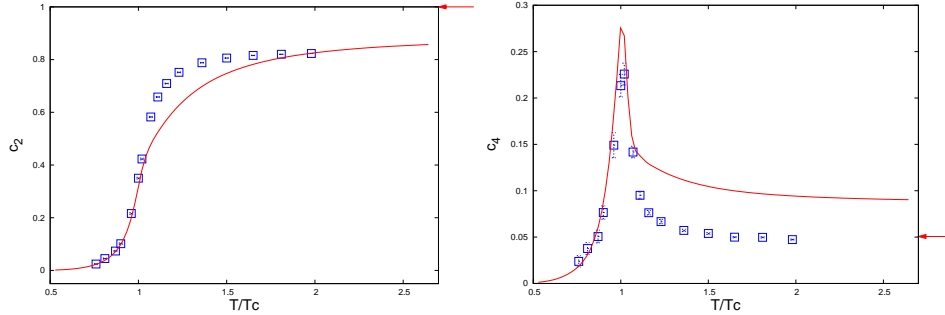


**Figure 2.** The QNS (left) and the fourth-order coefficient of reduced pressure (right) as a function of  $T/T_C$ . Symbols are lattice data. Arrows on the right indicate ideal gas values.

We study [41] some of the thermodynamic properties of strongly interacting matter using the Polyakov-loop + Nambu–Jona–Lasinio (PNJL) model [42]. The motivation behind the PNJL model is to couple the chiral and deconfinement order parameters inside a single framework. We have computed the EoS, the quark number susceptibilities, the specific heat  $C_v$ , the speed of sound (basically its square,  $v_s^2$ ), and the conformal measure  $\mathcal{C} = \Delta/\epsilon$ , where  $\Delta = \epsilon - 3P$  is the interaction measure and  $\epsilon$  and  $P$  are respectively the energy density and pressure of strongly interacting matter. Comparisons of these quantities with those obtained on the lattice were made.

We use the parametrization of the PNJL model as given in ref. [43]. For our results we shall present the quantities as a function of temperature in units of a cross-over temperature which is taken to be  $T_C = 227$  MeV.

We found the pressure to grow from almost zero at low temperatures to about 90% of its ideal gas value at  $2.5T_C$ . Left panel in figure 2 shows the variation of the quark number susceptibility (QNS), which is the second-order coefficient ( $c_2$ ) of reduced pressure ( $P/T^4$ ), with  $T/T_C$ . This shows an order parameter-like behavior. At higher temperatures  $c_2$  reaches almost 85% of its ideal gas value, consistent with lattice data. Similar behavior has been observed in another model study [44] using density-dependent quark mass model.

The fourth-order derivative  $c_4$ , which can then be thought of as the ‘susceptibility’ of  $c_2$  shows a peak at  $T = T_C$  (right panel of figure 2). Near the transition temperature  $T_C$ , the effective model should work well and we observe that the structure of  $c_4$  is quite consistent with lattice data. Just above  $T_C$  however, there is a significant difference between our results of  $c_4$  and that of ref. [3]. Note that in the SB limit both  $c_2$  and  $c_4$  have only fermionic contributions. We expect that because the coupling strength is still large in this temperature regime it is unlikely that  $c_4$  should go to the SB limit within  $T < 2.5T_C$ . Moreover, the quark masses used in ref. [3] is considerably large ( $m/T = 0.4$ ) to expect fermionic observables to go to the SB limit. However, it is possible that our overestimation is due to the use of mean-field approximation.

Left panel of figure 3 shows that  $C_v$  grows with increasing temperature and reaches a peak at  $T_C$ . For comparison, we have also plotted the values of  $4\epsilon/T^4$ , at which the specific heat is expected to coincide for a conformal gas.

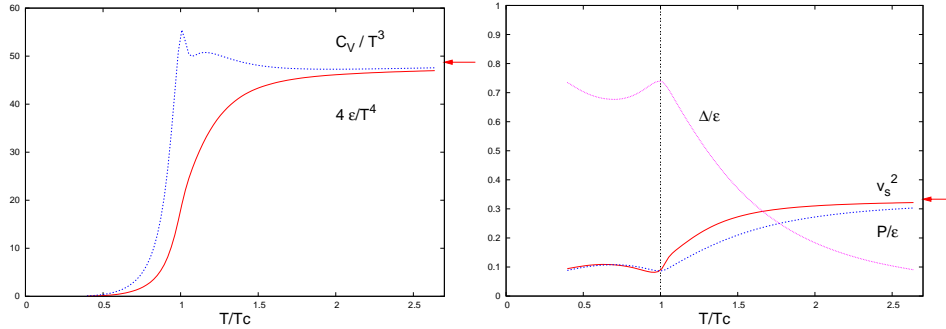


**Figure 3.**  $C_v/T^3$  and  $4\epsilon/T^4$  (left) and squared velocity of sound  $v_s^2$  and conformal measure  $\mathcal{C} = \Delta/\epsilon$  (right) as a function of  $T/T_C$ . The arrow on the right shows the ideal gas value.

We plot the speed of sound and conformal measure in the right panel of figure 3. The value of  $P/\epsilon$  matches with that of  $v_s^2$  for  $T < T_C$  and also goes close again above  $2.5T_C$ . But in between these two limits  $v_s^2$  is distinctly greater than  $P/\epsilon$ . Thus,  $\mathcal{C}$  would go to zero much faster if we replace  $P/\epsilon$  by  $v_s^2$  for computing  $\mathcal{C}$ . Near  $T_C$ ,  $v_s^2$  is minimum which goes close to 0.08.

The values for the conformal measure  $\mathcal{C}$  also closely resembles the lattice data of ref. [45]. The dip at temperatures less than  $T_C$  is prominent in both the cases. At even lower temperatures we find  $\mathcal{C}$  to increase. For a nonrelativistic ideal gas, the ratio of  $P/\epsilon$  should go to zero, and thus  $\mathcal{C}$  should then go to 1. On the other hand, at high temperatures either an ideal gas or a conformal behavior should be recovered for which  $\mathcal{C}$  should go to zero.

## 5. Possibility of bound states in QGP

*Sanjay K Ghosh, Munshi G Mustafa and Rajarshi Ray*

Recent LQCD calculations [6,7] suggest that pseudoscalars and vectors resonances may exist above  $T_C$ . Color bound states of parton at rest have been claimed by analyzing LQCD data [46]. The situation, however, changes if the test charge,  $Q^a$ , is in motion relative to the heat bath. The motion of the particle fixes the direction in space and spherical symmetry of the problem reduces to axial symmetry. This implies the loss of spherical symmetry of the Debye screening cloud around the moving test charge resulting in a wake in the induced charge due to dynamical screening [47]. The negative minimum found in the wake potential indicates an induced space-charge density of opposite sign. Thus, a particle moving relative to a particle in the induced space-charge density would constitute a dipole oriented along the direction of motion. We briefly describe the potential due to such a dipole interaction in QGP, details of which can be seen in ref. [47].

The spatial distribution of the scaled [47a] potential in cylindrical coordinates are displayed in figure 4 for two velocities. The left panel of figure 4 corresponds to  $v = 0.55c$  whereas the right panel is for  $v = 0.99c$ . The dipole potential shows

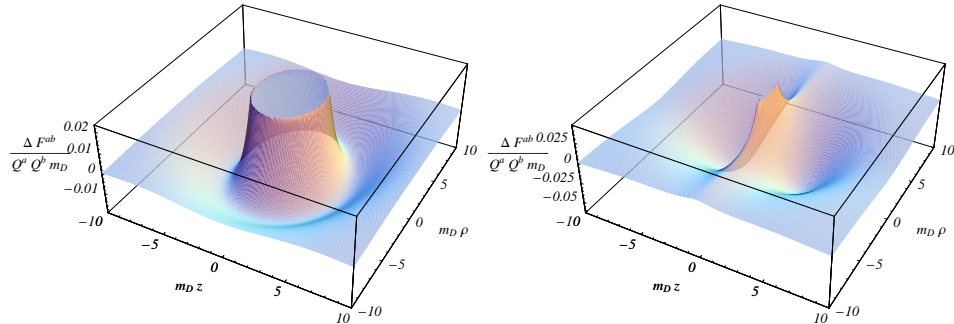


**Figure 4.** Left panel: Spatial distribution of the scaled dipole potential with respect to Debye screening mass  $m_D$  for  $v = 0.55c$ . Right panel: Same as left panel for  $v = 0.99c$ .

the usual singularity of the screening potential at  $r = 0$  ( $z = 0$  and  $\rho = 0$ ) and a completely symmetric behavior along with a pronounced negative minimum in the  $\rho$ - $z$  plane. This is due to the compensating effects between the electric and the magnetic interactions. For details of electric and magnetic interactions, readers are referred to [47]. With the increase of  $v$  the relative strength of the dipole potential grows strongly. For  $v = 0.99c$  a substantial repulsive interaction has grown in the transverse plane, i.e., in the direction of  $\rho$  but at  $z = 0$ , becoming responsible for a vertical split of the minimum in the  $\rho$ - $z$  plane. However, the general form of the potential mostly resembles the Lennard–Jones-type with a pronounced repulsive as well attractive parts.

In QCD the interaction between color charges in various channels is either attractive or repulsive. A quark and an antiquark yield the sum of irreducible color representations [47b]:  $\mathbf{3} \otimes \bar{\mathbf{3}} = \bar{\mathbf{1}} \oplus \mathbf{8}$ , with the interaction strength of the color singlet representation is  $-16/3$  (attractive) whereas that of the color octet channel is  $2/3$  (repulsive). Similarly, a two-quark state corresponds to the sum of the irreducible color representations:  $\mathbf{3} \otimes \mathbf{3} = \bar{\mathbf{3}} \oplus \mathbf{6}$ , where the antisymmetric color triplet is attractive ( $-8/3$ ) giving rise to possible bound states [46]. The symmetric color sextet channel, on the other hand, is repulsive ( $4/3$ ). Color bound states (i.e. diquarks) of partons at rest have been claimed by analyzing LQCD data [46]. The situation is different when partons are in motion. The dipole potentials along the direction of propagation and also normal to it have both attractive and repulsive parts, similar to the Lennard–Jones form. So, all the attractive channels or the repulsive channels in the static case get inverted due to the two comoving partons constituting a dipole in the QGP. This could lead to dissociation of bound states (or to resonance states) as well as formation of color bound states in the QGP.

Within our model such bound states as well as other colored binary states in the QGP can experience different potentials along the dipole direction and the direction normal to it. Along the direction of motion, binary states which were bound in QGP may become resonance states or dissociate beyond  $T_C$ . Similarly, those colored states which were not bound initially in the QGP, may transform into bound states. There are some long distance correlations among partons in the QGP, which could indicate the appearance/disappearance of binary states in the

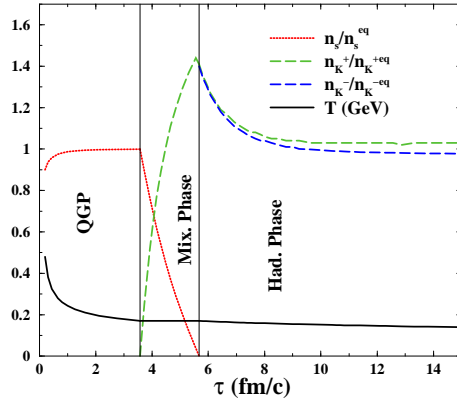


**Figure 5.** Evolution of strange particles and temperature when  $T_C = 170$  MeV.  $n_i/n_i^{\text{eq}}$  is the ratio of the no. density of  $i$ -type particle.

QGP beyond  $T_C$ . The temperature up to which they survive need further analysis of the bound state properties in detail, which was initiated during WHEPP-09 and some progress has been made. The complete work will be reported elsewhere.

## 6. $\phi$ -production at RHIC

*Jajati K Nayak, Jan-e Alam, Bedangadas Mohanty, Pradip Roy, Abhee K Dutt-Mazumder*

Among the promising signals to analyse the matter formed in relativistic heavy-ion collision, the study of strangeness is an important one. The production and evolution of strange particles give good information about the formation of QGP.  $\phi$  meson is a bound state of strange quark ( $s$ ) and anti-strange quark ( $\bar{s}$ ). The interaction of  $\phi$  meson with nuclear matter is suppressed according to Okubo–Zweig–Izuka (OZI) rule.  $\phi$  meson after its production during hadronization suffers less rescattering with hadronic matter. So it gives thermodynamic information of the state of matter during hadronization stage. From the  $\phi$  spectra at  $\sqrt{s} = 200$  GeV (RHIC energy) we extract the information about critical temperature  $T_C$  of the quark-hadron phase transition.

We assume a first-order quark-hadron phase transition for  $\sqrt{s} = 200$  GeV. In QGP phase  $s$  and  $\bar{s}$  quarks are produced mainly by gluon–gluon fusion and annihilation of light quarks and anti-quarks. These  $s$  and  $\bar{s}$  form  $\phi$  through hadronization process. This production is not OZI suppressed. We expect excess  $\phi$  mesons if QGP is formed in the initial state of heavy-ion collisions as compared to a hadronic initial state. The production of  $\phi$  from sources other than plasma is very small.  $\phi$  spectra is experimentally reconstructed from kaons since it decays to  $K^+$  and  $K^-$ . Although  $K^+$  and  $K^-$  carry some scattering effects still  $\phi$  meson spectra give reliable information of the thermodynamic state of matter during its formation.

We calculate the ratio of the multiplicity of  $\phi$  meson to the total multiplicity at midrapidity of RHIC experiment from thermal model. The ratio depends on

the critical temperature  $T_C$  and the effective degeneracy  $g_{\text{eff}}$ . We took this value from lattice QCD calculation. We found the measured value to be more than the calculated one. This is expressed as an overproduction or enhancement factor  $\gamma_\phi$ . To know where and when this overproduction occurs we adopted Boltzmann equation and solved for the evolution of strange particles (e.g.,  $s, \bar{s}, K^+, K^-$  etc.) in QGP, mixed and hadron phases. With proper initial conditions from hadron spectra we solved the Boltzmann equation and temperature evolution equation and found the overproduction factor  $\gamma_\phi \sim r_{K^+}^2 = 1.63$  ( $r_{K^+}$  being the ratio of nonequilibrium to equilibrium density of  $K^+$  as shown in figure 5) when  $T_C = 170$  MeV. The production of  $K^+$  is restricted by a parameter  $\delta$ . At best half of the strange quarks can go to the  $K^+$ . This is expressed as  $\delta = 0.5$ . So this puts the limit on the critical temperature, i.e.  $T_C > 170$  MeV. Similarly a limit on  $g_{\text{eff}}$  also has been put [48].

## 7. AdS/CFT $\rightarrow$ QCD/QGP?

Balram Rai

The idea that QGP at RHIC,  $T \sim 2T_C$ , seems to be in a strongly coupled regime (interaction energy  $\gg$  kinetic energy) has presently been attracted a lot of attention:

1. The equation of states obtained in LQCD deviates from ideal gas behavior. Combining the LQCD data on quasi-particle masses and interparticle potential one indeed finds [46] a lot of bound states and resonances above  $T_C$ . This could be an explanation for charmonium states remaining bound up to  $(2-3)T_C$ , as was directly observed on lattice [6]. However, resonances above  $T_C$  due to marginal bound states give rise to large cross-section and small mean free path leading to collective flow.
2. Collective phenomena observed at RHIC lead to view QGP as a near perfect fluid [13]. The deviation of elliptic flow data from the prediction of hydrodynamic calculations only occur at  $p_T \sim 1.5-2$  GeV/c and this leads to viscosity-to-entropy ratio,  $\eta/s \sim 0.1-0.2$ , which is more than an order of magnitude less than that in pQCD.
3. The charm diffusion constant [49] deduced from the single electron data and elliptic flow is also an order of magnitude less than pQCD estimates.
4. The interaction parameter  $\Gamma = \langle \text{potential energy} \rangle / T$  is obviously not small for QGP [50]. At such  $\Gamma$  the classical strongly coupled plasma is a good liquid.

As seen the pQCD calculations of transport coefficients are not reliable around and above  $T_C$ , which is believed to be in strong coupling regime. On the other hand, the LQCD is a rigorous calculational method applicable in hot, strongly coupled, gauge theory. Because it is formulated in Euclidean space, it is well-suited for computing static thermodynamic quantities and less well-suited for transport coefficients, or dynamical processes of any sort. Complementary nonperturbative techniques are thus desirable. One such technique is the anti-de Sitter/conformal field theory (AdS/CFT) correspondence, which maps nonperturbative problems in certain hot strongly coupled gauge theories onto calculable problems in a dual gravity theory [51]. This method has been applied to calculate the shear viscosity [52]

in  $\mathcal{N} = 4$  supersymmetric Yang–Mills (SYM) theory which gives an upper bound of  $\eta/s \sim 1/4\pi$ , close to the RHIC value. Also effort [53] was made to compute certain diffusion coefficients in the same spirit. The ratio of pressure to that of Stefan–Boltzmann limit in  $\mathcal{N} = 4$  SYM is remarkably close to the corresponding ratio in LQCD at temperatures a few times  $T_C$  where it is strongly coupled [54].

Usually the properties of  $\mathcal{N} = 4$  SYM theory are completely different from QCD. The former one is a conformal theory with no particle spectrum or  $\mathcal{S}$ -matrix, whereas the latter one is a confining theory with a realistic particle interpretation. In view of this, members of this working group were interested to know the basics of AdS/CFT correspondence to supersymmetric gauge theories in strong coupling limit and their connection to QCD/QGP. Balram Rai delivered two comprehensive lectures on this topic in a very elementary level, which are discussed below in brief.

- $\mathcal{N} = 4$  SYM is a conformally invariant theory with two parameters: the rank of the gauge group  $N_C$  and the t’Hooft coupling  $\lambda = g_{YM}^2 N_C$  where  $g_{YM}$  is the Yang–Mills coupling. Its on-shell field content includes eight bosonic and eight fermionic degrees of freedom, all in color adjoint representation.
- Basic argument leading to this correspondence: Consider in Type-IIB string theory, a configuration of  $N_C$   $D3$ -branes stacked on top of each other. The appropriate theory living on the branes is  $\mathcal{N} = 4$  SYM theory. On the other hand, if  $N_C$  is large, the stack of  $D3$ -branes has large tension, which curves space–time. In the limit of large t’Hooft coupling  $\lambda$ , the brane geometry has small curvature and can be described by supergravity. Therefore, one can have two descriptions of the same physics in terms of strongly coupled gauge theory on the branes and classical gravity on a certain background.
- AdS/CFT conjecture (or gauge/string duality) states that this theory is exactly equivalent to Type-IIB string theory in an  $AdS_5 \times S^5$  gravitational background, where  $AdS_5$  is the five-dimensional anti-de Sitter space and  $S^5$  is the five-dimensional sphere. At large  $N_C$  and large  $\lambda$ , the string theory can be approximated by classical Type-IIB supergravity.
- The above approximation permits nonperturbative calculations in quantum field theory mapped into problems in classical general relativity. In this context, raising the temperature of the gauge theory corresponds to a black hole (or a black brane) into the center of  $AdS_5$ . According to AdS/CFT, the Hawking temperature of the black hole becomes the temperature of the gauge theory.
- Even at  $T = 0$ , the  $\mathcal{N} = 4$  SYM theory is a conformal one whereas the QCD is a confining theory, but at  $T \neq 0$  both theories describe hot, nonabelian plasmas with Debye screening, finite spatial correlation length, and qualitatively similar hydrodynamic behavior. The major difference is that all the excitations (quarks, gluons and scalars) in  $\mathcal{N} = 4$  SYM plasma are in adjoint representation, while hot QCD plasma has quarks in fundamental and gluons in adjoint representations. This leads to an assumption that the fundamental representation fields have negligible influence on bulk properties of the plasma. One may view the quarks as test particles which serve as probes of dynamical processes in the background of  $\mathcal{N} = 4$  plasma.
- As found, the shear viscosity, the thermodynamic quantities such as pressure, energy density, entropy etc. computed in  $\mathcal{N} = 4$  SYM in strong coupling

limits (large  $N_C$  and large  $\lambda$ ) are insensitive to details of the plasma composition or the precise interaction strength. These values are remarkably close to those properties of QGP observed in RHIC and obtained LQCD.

- These observations have led us to think of a connection of AdS/CFT gravity dual to RHIC collisions!

## 8. Neutrino emission rates in crystalline color superconducting quark matter

*Prashanth Jaikumar, Hiranmaya Mishra and Andreas Schmitt*

The existence of deconfined quark matter inside compact stars can be verified if the stellar cooling rate is found to be substantially different from the neutron stars, and can be attributed directly to the neutrino emission rates of (superconducting) quark matter. This requires [54a]: (1) identifying the ground state of dense QCD at intermediately large quark chemical potentials ( $\mu_q \sim 300\text{--}400$  MeV) that characterize the interior of neutron stars and (2) computing the neutrino emission rate and specific heat of this phase to determine its cooling behavior.

One possible manifestation of the diquark phase at intermediate densities, where the strange quark mass is large, is a crystalline color superconductor in which quarks with different Fermi surfaces pair at nonzero momentum, resulting in an inhomogeneous but spatially periodic order parameter [55]. This phase spontaneously breaks translation and rotational symmetries, and the free energy of the system is minimized when the gap varies spatially in accordance with the residual discrete symmetries of this phase. This is the QCD incarnation of the LOFF (Larkin–Ovchinnikov–Fulde–Ferrell) phase in electronic spin systems.

The presence of color superconducting phases is expected to alter the cooling behavior of neutron stars. The equation that determines the cooling of an isothermal neutron star of volume  $V$  in global heat balance is

$$c_v \frac{dT}{dt} = -L_\nu \equiv -\epsilon_\nu V, \quad (3)$$

where  $T$  is the temperature,  $t$  is the time,  $\epsilon$  is the neutrino emissivity and  $c_v$  is the specific heat at constant volume  $V$  of the quark phase.

Minimization of the thermodynamic potential leads to the nonisotropic gap equation [56]

$$\Delta = \frac{2G}{(2\pi)^3} \int dp \frac{2 \sin^2(\beta/2)}{\sqrt{(|q+p| + |q-p| - \bar{\mu})^2 + 4\Delta^2 \sin^2(\beta/2)}}, \quad (4)$$

where the momentum integration runs over the pairing region defined by the domain  $\{\mathcal{P} : \mathbf{p} | E_1(p) > 0, E_2(p) > 0\}$ . Here, the angle  $\beta$  is the angle between the up-quark momentum ( $q+p$ ) and the down-quark momentum ( $q-p$ ). Further, the quasi-particle energies are given as [57]

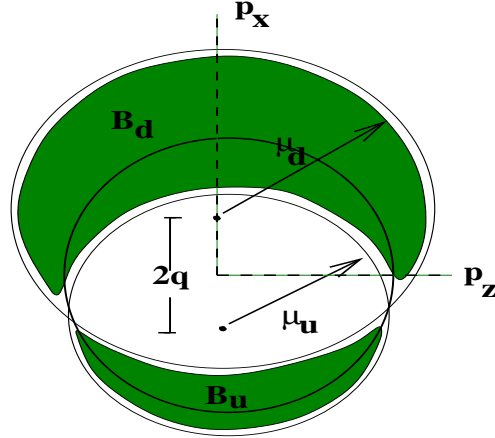


**Figure 6.** Allowed (unshaded) and blocked (shaded) regions for pairing between up and down-quarks in the LOFF phase. The two-dimensional projection of the Fermi spheres for the two flavors of quark are shown displaced by an amount  $2\mathbf{q}$ . The dispersion  $E_1(E_2)$  vanishes on the boundary of the lower (upper) banana-shaped region. These surfaces make the principal contributions to the specific heat and neutrino emissivity. Particle-hole pairing occurs on the boundary of the elliptical region but is clearly disfavored at low temperatures.

$$E_1(p) = \delta\mu + \frac{1}{2}(|p+q| - |p-q|) + \frac{1}{2}\sqrt{(|q+p| + |q-p| - 2\bar{\mu})^2 + 4\Delta^2 \sin^2(\frac{1}{2}\beta)} \quad (5)$$

and

$$E_2(p) = -\delta\mu - \frac{1}{2}(|p+q| - |p-q|) + \frac{1}{2}\sqrt{(|q+p| + |q-p| - 2\bar{\mu})^2 + 4\Delta^2 \sin^2(\frac{1}{2}\beta)}. \quad (6)$$

In the above,  $\bar{\mu} = (\mu_u + \mu_d)/2$  and  $\delta\mu = \mu_d - \mu_u$  are the average and the difference respectively of the chemical potentials of the two condensing quarks. Thus, crystalline superconductivity is characterized by dispersion relations which vary with the direction of momentum, yielding gaps which vary from zero up to a maximum of  $\Delta$ .

For the purpose of neutrino emissivity calculations, it is the nodal surfaces described by  $E_1 = 0$  and  $E_2 = 0$  that make dominant contributions to the phase-space integral in eq. (7). Thus one needs to know the dispersion relation near the ‘blocking’ regions  $B_u, B_d$  in figure 6, whose boundary can be specified by solving  $E_i(p) = 0$  for the angle between the condensate momentum  $q$  and the relative momentum between the pairing quarks  $p$ .

**Table 1.**

$c_\nu$	0	1	2
Linear	$T^3$	$\bar{\mu}T^2$	$\bar{\mu}^2T$
Quadratic	$\bar{\mu}T^2$	$\bar{\mu}^{3/2}T^{3/2}$	$\bar{\mu}^{5/2}T^{1/2}$

The neutrino emissivity is calculated from

$$\epsilon_\nu = \left[ \prod_{i=1}^4 \int_{E(p_i)=0} \frac{d^3 p_i}{(2\pi)^3} \right] E_\nu W n(p_d)(1 - n(p_u))(1 - n(p_e)) \times \psi_d(p_d)^2 B \psi_u(p_u)^2, \tag{7}$$

where  $i = 1, \dots, 4$  represents  $d, u, e, \nu$  respectively.

$$W = \frac{(2\pi)^2 \delta^4(p_d - p_u - p_e - p_\nu)}{\prod_{i=1}^4 2E_i} |M|^2 \tag{8}$$

with  $|M|^2 = 64G_F^2 \cos^2 \theta_C (p_d \cdot p_\nu)(p_u \cdot p_e)$  being the matrix element for the weak interaction process. The  $\psi$ 's are Bogoliubov coefficients for the  $(du)$  quasi-particles.

The specific heat can be calculated from

$$c_\nu = \frac{1}{T^2} \int \frac{d^3 p}{(2\pi)^3} \frac{E(p)^2}{(e^{E(p)/T} + 1)(e^{-E(p)/T} + 1)}. \tag{9}$$

Since we are interested in the low-temperature behavior of the specific heat, we can approximate

$$c_\nu \approx \frac{1}{T^2} \int \frac{d^3 p}{(2\pi)^3} E(p)^2 e^{-E(p)/T}. \tag{10}$$

The temperature dependence of the specific heat can be classified with respect to the behavior of the dispersion relations in the vicinity of its zeros and the dimension  $d = 0$  (point), 1 (line) and 2 (surface) of the sub-manifold where the dispersion vanishes. Using the above formula, we can deduce the results for the temperature dependence of the specific heat (see table 1) where constants of proportionality of order one have been omitted. These relations indicate that the circle of nodes at the tips of the two banana-shaped regions contribute the most to the specific heat since  $\bar{\mu} \gg T$ . The point nodes contribute less to the specific heat but will dominate the contribution to the neutrino emissivity since their phase-space weights are larger. The computation for the emissivity is complicated by the need to perform a bounded phase-space integration excluding the blocking regions, and this will be attempted numerically.

References

- [1] E V Shuryak, *Sov. Phys. JETP* **47**, 212 (1978)
- [2] E Laermann and O Philipsen, *Ann. Rev. Nucl. Part. Sci.* **53**, 163 (2003)
- [3] C R Allton *et al*, *Phys. Rev.* **D71**, 054508 (2005)
- [4] R V Gavai and S Gupta, *Phys. Rev.* **D72**, 054006 (2005)
- [5] A Nakamura and S Sakai, *Phys. Rev. Lett.* **94**, 072305 (2005)
- [6] S Datta, F Karsch, P Petreczky and I Wetzorke, *Phys. Rev.* **D69**, 094507 (2004)
- [7] F Karsch, E Laermann, P Petreczky, S Stickan and I Wetzorke, *Phys. Lett.* **B530**, 147 (2002)  
F Karsch, *Nucl. Phys.* **A715**, 701 (2003)
- [8] PHENIX Collaboration: S S Adler *et al*, *Phys. Rev.* **C69**, 034909 (2004)
- [9] PHENIX Collaboration: K Adcox *et al*, *Phys. Rev. Lett.* **89**, 212301 (2002)  
PHENIX Collaboration: S S Adler *et al*, *Phys. Rev. Lett.* **91**, 182301 (2003)
- [10] PHENIX Collaboration: S S Adler *et al*, *Phys. Rev. Lett.* **91**, 072301 (2003)
- [11] PHENIX Collaboration: K Adcox *et al*, *Phys. Rev. Lett.* **88**, 022301 (2002)  
STAR Collaboration: C Adler *et al*, *Phys. Rev. Lett.* **89**, 202301 (2002); *ibid.* **90**, (2003) 032301; *ibid.* **90**, 082302 (2003)  
PHOBOS Collaboration: B B Back *et al*, *Phys. Lett.* **B578**, 297 (2004)  
STAR Collaboration: J Adams *et al*, *Phys. Rev. Lett.* **91**, 172302 (2003)  
STAR Collaboration: C Adler *et al*, *Phys. Rev. Lett.* **90**, 082302 (2003)
- [12] M Gyulassy and M Plümer, *Phys. Lett.* **B243**, 432 (1990)  
J D Bjorken, preprint FERMILAB-PUB-82-059-THY  
M H Thoma and M Gyulassy, *Nucl. Phys.* **B351**, 491 (1991)  
E Braaten and M H Thoma, *Phys. Rev.* **D44**, 1298 (1991)
- [13] D Teaney, J Lauret and E V Shuryak, *Phys. Rev. Lett.* **86**, 4783 (2001)  
P F Kolb, P Huovinen, U Heinz and H Heiselberg, *Phys. Lett.* **B500**, 232 (2001)  
A K Chaudhuri, nucl-th/0604014
- [14] M Gyulassy, P Levai and I Vitev, *Phys. Lett.* **B538**, 282 (2002)  
M Gyulassy, I Vitev and X N Wang, *Phys. Rev. Lett.* **86**, 2537 (2001)  
X-N Wang and M Gyulassy, *Phys. Rev.* **D44**, 3501 (1991)  
M Gyulassy and X-N Wang, *Nucl. Phys.* **B420**, 583 (1994)  
X-N Wang, M Gyulassy and M Plumer, *Phys. Rev.* **D51**, 3436 (1995)
- [15] C A Salgado and U A Wiedemann, *Phys. Rev. Lett.* **89**, 092303 (2002)  
C A Salgado and U A Wiedemann, *Phys. Rev. Lett.* **93**, 042301 (2004)  
E Wang and X N Wang, *Phys. Rev. Lett.* **89**, 162301 (2002)  
R Baier, Y L Dokshitzer, A H Mueller and D Schiff, *J. High Energy Phys.* **0109**, 033 (2001)  
E V Shuryak, *Phys. Rev.* **C66**, 027902 (2003)
- [16] B G Zakharov, *JETP Lett.* **63**, 952 (1996); **64**, 781 (1996); **65**, 615 (1997); **70**, 176 (1999); **73**, 49 (2001)
- [17] B Müller, *Phys. Rev.* **C67**, 061901(R) (2003)
- [18] M G Mustafa and M H Thoma, *Acta Phys. Hung.* **A22**, 93 (2005)  
M G Mustafa, *Phys. Rev.* **C72**, 014905 (2005)  
J Alam, P Roy and A K Dutt-Mazumder, hep-ph/0604131  
A K Dutt-Mazumder, J Alam, P Roy and B Sinha, *Phys. Rev.* **D71**, 094016 (2005)
- [19] S S Adler *et al*, *Phys. Rev. Lett.* **94**, 232301 (2005)
- [20] S A Bass, B Müller and D K Srivastava, *Phys. Rev. Lett.* **90**, 082301 (2003)  
R J Fries, B Müller and D K Srivastava, *Phys. Rev. Lett.* **90**, 132301 (2003)  
J Alam *et al*, nucl-th/0508043

- [21] L Kluberg, *Eur. Phys. J.* **C43**, 145 (2005)
- [22] NA50 Collaboration: M C Abreu *et al*, *Phys. Lett.* **B553**, 167 (2003)  
 NA50 Collaboration: B Alessandro *et al*, *Eur. Phys. J.* **C33**, 31 (2004)  
 NA50 Collaboration: G Borges *et al*, *Eur. Phys. J.* **C43**, 161 (2005)
- [23] NA50 Collaboration: B Alessandro *et al*, *Eur. Phys. J.* **C39**, 335 (2005)  
 NA50 Collaboration: L Ramello, *Proc. Quark Matter 2005*, <http://qm2005.kfki.hu>
- [24] NA60 Collaboration: E Scomparin, *Proc. Quark Matter 2005*, <http://qm2005.kfki.hu>  
 NA60 Collaboration: R Arnaldi, *Proc. QM 2005*, <http://qm2005.kfki.hu>
- [25] V Tram, presentation at CERN Heavy Ion Forum, 6 October 2006
- [26] H Satz *et al*, *Eur. Phys. J.* **C32**, 547 (2004)
- [27] R Rapp *et al*, *Nucl. Phys.* **A715**, 545 (2003); *Phys. Rev. Lett.* **92**, 212301 (2004)
- [28] A Capella *et al*, *Eur. Phys. J.* **C42**, 419 (2005)
- [29] A P Kostyuk *et al*, *Phys. Rev.* **C68**, 041902 (2003)
- [30] J G Contreras, M Lopez Noriega and A Morsch, Jet reconstruction in Pb–Pb collisions with the ALICE detector ALICE Internal Note ALICE-INT-2005-035; ALICE Collaboration, ALICE Physics Performance Report, Vol. 2, CERN/LHC 2005-030 (2005), submitted to *J. Phys. G*.
- [31] S-L Blyth, Jet studies in ultra-relativistic heavy-ion collisions with the ALICE detectors at the LHC; MSc. Thesis, nucl-ex/0510065 (2005)  
 S-L Blyth *et al*, A universal jet finding algorithm for heavy-ion collisions at the LHC applied to the ALICE experiment, submitted to *Nucl. Instrum. Methods* (2005)
- [32] N Borghini, P M Dinh and J-Y Ollitrault, *Phys. Rev.* **C64**, 054901 (2001)
- [33] S C Phatak and P K Sahu, *Phys. Rev.* **C69**, 024901 (2004)
- [34] X-N Wang and M Gyulassy, *Phys. Rev.* **D45**, 844 (1992)
- [35] R Baier, A H Mueller, D Schiff and D T Son, *Phys. Lett.* **B502**, 51 (2001); *ibid.* **B539**, 46 (2002)
- [36] R S Bhalerao, J-P Blaizot, J-Y Ollitrault, *Phys. Lett.* **B627**, 49 (2005)
- [37] STAR Collaboration: J Adams *et al*, *Phys. Rev.* **C72**, 014904 (2005)
- [38] S Ejiri, F Karsch and K Redlich, *Phys. Lett.* **B633**, 275 (2005)
- [39] J Liao and E Shuryak, *Phys. Rev.* **D73**, 014509 (2006)
- [39a] The authors are thankful to Rajiv Gavai for useful discussion during WHEPP-09 where this work was initiated. Full details of this work was reported in hep-ph/0603050 and published in *Phys. Rev.* **D73**, 114007 (2006)
- [40] L D McLerran and B Svetitsky, *Phys. Rev.* **D24**, 450 (1981)
- [41] S K Ghosh, T K Mukherjee, M G Mustafa and R Ray, *Phys. Rev.* **D73**, 114007 (2006); hep-ph/0603050
- [42] P N Meisinger and M C Ogilvie, *Phys. Lett.* **B379**, 163 (1996); *Nucl. Phys. (Proc. Suppl.)* **B47**, 519 (1996)
- [43] C Ratti, M A Thaler and W Weise, *Phys. Rev.* **D73**, 014019 (2006)
- [44] S K Ghosh, T K Mukherjee and S Raha, nucl-th/0509086, *Mod. Phys. Lett.* **A21**, 2067 (2006)
- [45] R V Gavai, S Gupta and S Mukherjee, hep-lat/0506015
- [46] E V Shuryak and I Zahed, *Phys. Rev.* **D70**, 054507 (2004)
- [47] M G Mustafa, M H Thoma and P Chakraborty, *Phys. Rev.* **C71**, 017901 (2005)  
 P Chakraborty, M G Mustafa and M H Thoma, hep-ph/0606316, *Phys. Rev. D* (2006) in press
- [47a] The potential is scaled with the screening mass  $m_D$  as well as with the interaction strength,  $Q^a Q^b$ . So, the details of the potential will depend on the temperature, the strong coupling constant and the sign of the interaction strength [47]
- [47b] Their strength of the color interaction [46] can be calculated using  $SU(3)$  color group

*Heavy-ion physics and QGP*

- [48] J K Nayak, J Alam, B Mohanty, P Roy and A K Dutt-Mazumder, nucl-th/0509061
- [49] G D Moore and D Teaney, *Phys. Rev.* **C71**, 064904 (2005)  
H van Hees and R Rapp, *Phys. Rev.* **C71**, 034907 (2005)  
H van Hees, V Greco and R Rapp, *Phys. Rev.* **C73**, 034913 (2006)
- [50] M H Thoma, *J. Phys.* **G31**, L7 (2005); *Phys. Rev.* **D72**, 094030 (2005)
- [51] J M Maldacena, *Adv. Theor. Math. Phys.* **2**, 231 (1998)  
E Witten, *Adv. Theor. Math. Phys.* **2**, 505 (1998)  
S S Gubser, I R Klebanov and A M Polyakov, *Phys. Lett.* **B428**, 105 (1998)
- [52] G Policastro, D T Son and A O Starinets, *Phys. Rev. Lett.* **87**, 081601 (2001)  
A Buchel, J T Liu, *J. High Energy Phys.* **0311**, 031 (2003); *Phys. Rev. Lett.* **93**, 090602 (2004)
- [53] G Policastro, D T Son and A O Starinets, *J. High Energy Phys.* **0209**, 43 (2002)
- [54] S S Gubser, I R Klebanov and A A Tseytlin, *Nucl. Phys.* **B499**, 217 (1999)
- [54a] This work was initiated during WHEPP-09 and substantial progress has already been made
- [55] M Alford, J Bowers and K Rajagopal, *Phys. Rev.* **D63**, 074016 (2001)
- [56] J Bowers, J Kundu, K Rajagopal and E Shuster, *Phys. Rev.* **D64**, 014024 (2001)
- [57] J Bowers (2003) PhD Thesis, 180 pages